Phys. Oceanogr., Vol. 10, No. 6, pp. 503–512 (1999)

Generation of internal waves by a barotropic tide in the coastal zone*

S. V. DOVGAYA and L. V. CHERKESOV

Abstract — Within the framework of the linear theory of long waves, we study internal waves generated by a barotropic tide in a two-layer ocean of variable depth taking into account the influence of the Coriolis force. Barotropic waves run over an extended unevenness of the bottom at an arbitrary angle. This unevenness is regarded as a model of the continental slope and shelf. We establish the dependences of the amplitudes of generated internal waves on the angle of incidence of the barotropic tide, topography of the bottom, and stratification.

The mathematical simulation of wave processes in the zones of extended inhomogeneities of the bottom topography is an important scientific problem. Thus, the wave motions induced by a barotropic tide climbing along the normal to the axis of an extended unevenness of the bottom topography were studied in [1–3]. Several analytic solutions are also known for the case of a barotropic tide running at an arbitrary angle over extended ridges in a homogeneous fluid [4, 5]. However, for practical purposes, it is necessary to have more exact approximations of stratification of the fluid and the bottom topography aimed at subsequent application of numerical methods. In this connection, in [6, 7], within the framework of a two-layer model, we considered wave motions of a fluid above ridges whose topography is close to the actual. In the present work, on the basis of the linear theory of long waves in a fluid with jump of density, we make an attempt to study internal waves generated by a barotropic tide running over the continental slope and shelf.

1. We consider a basin unbounded in horizontal directions and filled with a two-layer fluid (Fig. 1a). In the upper layer of constant depth h_1, the density of the fluid is equal to ρ_1, whereas in the lower layer of variable depth, it is equal to ρ_2 ($\rho_2 > \rho_1$). In regions I ($x < -l_1$) and III ($x > l_2$), the depth of the basin is constant ($H_1 = h_1 + h_2$ and $H_3 = h_1 + h_4$, respectively). In region II ($-l_1 \le x \le l_2$), the depth is variable ($H_2 = h_1 + h_3(x)$). In the first region, the barotropic wave

$$\zeta = A_1 \exp\left[i(k_1 x + ny - \sigma t)\right] \tag{1}$$

propagates at an angle α to the x–axis.

We determine the characteristics of wave perturbations caused by wave (1) de-

* Translated by Peter V. Malyshev and Dmitry V. Malyshev
UDC 532.59

pending on the direction of its propagation ($\tan\alpha = n/k_1$), geometry of the bottom, and stratification (Fig. 1b).

Assume that the fluid is inviscid and wave perturbations are weak. Then, within the framework of the linear theory of long waves, the system of equations describing the motion of fluid in the region $x < -l_1$ takes the form [8]

$$\frac{\partial u_1}{\partial t} - f v_1 = -g\frac{\partial \zeta_1}{\partial x}, \qquad \frac{\partial v_1}{\partial t} + f u_1 = -g\frac{\partial \zeta_1}{\partial y},$$

$$h_1\left(\frac{\partial u_1}{\partial x} + \frac{\partial v_1}{\partial y}\right) = \frac{\partial \zeta_2}{\partial t} - \frac{\partial \zeta_1}{\partial t},$$

$$\frac{\partial u_2}{\partial t} - f v_2 = -g\left(\frac{\rho_1}{\rho_2}\frac{\partial \zeta_1}{\partial x} + \frac{\rho_2 - \rho_1}{\rho_2}\frac{\partial \zeta_2}{\partial x}\right), \tag{2}$$

$$\frac{\partial v_2}{\partial t} + f u_2 = -g\left(\frac{\rho_1}{\rho_2}\frac{\partial \zeta_1}{\partial y} + \frac{\rho_2 - \rho_1}{\rho_2}\frac{\partial \zeta_2}{\partial y}\right),$$

$$\frac{\partial (h_2 u_2)}{\partial x} + h_2\frac{\partial v_2}{\partial y} = -\frac{\partial \zeta_2}{\partial t}.$$

In regions II and III, the system has the same form but h_2 should be replaced by h_3 and h_4, respectively. Subscripts 1 and 2 of the quantities u, v, and ζ correspond to the upper and lower layers, respectively.

Since the incident wave is periodic with frequency σ and the coefficients in the system of equations (2) are independent of t and y, we seek the required solutions as functions periodic in the spatial coordinate y and t, namely,

$$\{\zeta_j, u_j, v_j\} = \{\bar{\zeta}_j, \bar{u}_j, \bar{v}_j\}(x)\exp[i(ny - \sigma t)]. \tag{3}$$

If we now substitute (3) in equations (2), then we get the following equation for the determination of ζ_1 in regions I and III (here and in what follows, the bars over ζ_j, u_j, and v_j, $j = 1, 2$, are omitted):

$$\frac{d^4\zeta_1}{dx^4} - \left(2n^2 - \frac{(h_1 + h_m)(\sigma^2 - f^2)}{g\varepsilon h_1 h_m}\right)\frac{d^2\zeta_1}{dx^2}$$

$$+ \left(n^4 - \frac{(h_1 + h_m)(\sigma^2 - f^2)}{g\varepsilon h_1 h_m}n^2 + \frac{(\sigma^2 - f^2)^2}{g\varepsilon h_1 h_m}\right)\zeta_1 = 0, \tag{4}$$

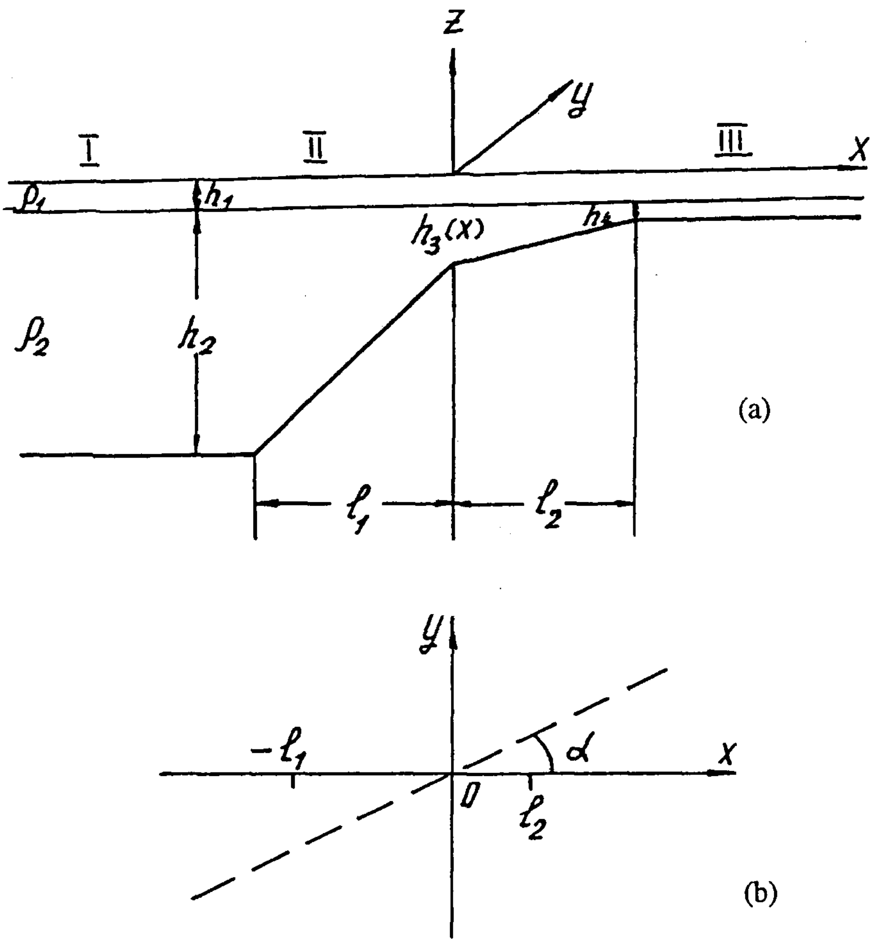

Figure 1. Schematic diagrams of the basin (a) and the direction of propagation of waves (b).

where $\varepsilon = (\rho_2 - \rho_1)/\rho_2$, $m = 2$ corresponds to region I, and $m = 4$ to region III. In the second region, for ζ_1, we have the following fourth-order ordinary differential equation with variable coefficients:

$$\frac{d^4\zeta_1}{dx^4} + \frac{1}{h_3}\frac{dh_3}{dx}\frac{d^3\zeta_1}{dx^3} - \left[2n^2 + \frac{nf}{\sigma h_3}\frac{dh_3}{dx} - \frac{(\sigma^2 - f^2)(h_1 + h_3)}{h_1 h_3 \varepsilon g}\right]\frac{d^2\zeta_1}{dx^2}$$

$$- \left(\frac{n^2}{h_3} - \frac{\sigma^2 - f^2}{h_1 h_3 \varepsilon g}\right)\frac{dh_3}{dx}\frac{d\zeta_1}{dx} + \left[n^4 + \frac{n^3 f}{\sigma h_3}\frac{dh_3}{dx}\right.$$

$$- \frac{n^2(\sigma^2 - f^2)(h_1 + h_3)}{h_1 h_3 \varepsilon g} - \frac{nf(\sigma^2 - f^2)}{\sigma h_1 h_3 \varepsilon g}\frac{dh_3}{dx} + \frac{(\sigma^2 - f^2)^2}{h_1 h_3 \varepsilon g^2}\Bigg]\zeta_1 = 0. \quad (5)$$

In this case, the components of the horizontal velocity in the upper and lower layers and the displacement of the interface of layers from its nonperturbed state are expressed via ζ_1 as follows:

$$u_1 = \frac{ig}{\sigma^2 - f^2}\left[-\sigma\frac{d\zeta_1}{dx} + nf\zeta_1\right], \qquad v_1 = -\frac{g}{\sigma^2 - f^2}\left[f\frac{d\zeta_1}{dx} - n\sigma\zeta_1\right],$$

$$u_2 = -\frac{ig}{\sigma^2 - f^2}\left[\sigma\frac{d\zeta_1}{dx} - fn\zeta_1 + \frac{\varepsilon h_1 g}{\sigma^2 - f^2}\left(\sigma\left(\frac{d^3\zeta_1}{dx^3} - n^2\frac{d\zeta_1}{dx}\right) - f\left(-n^3\zeta_1 + n\frac{d^2\zeta_1}{dx^2}\right)\right)\right],$$

$$v_2 = -\frac{g}{\sigma^2 - f^2}\left[f\frac{d\zeta_1}{dx} - n\sigma\zeta_1 + \frac{\varepsilon h_1 g}{\sigma^2 - f^2}\left(f\left(\frac{d^3\zeta_1}{dx^3} - n^2\frac{d\zeta_1}{dx}\right) + \sigma\left(n^3\zeta_1 - n\frac{d^2\zeta_1}{dx^2}\right)\right)\right],$$

$$\zeta_2 = \frac{h_1 g}{\sigma^2 - f^2}\frac{d^2\zeta_1}{dx^2} + \zeta_1\left(1 - \frac{n^2 h_1 g}{\sigma^2 - f^2}\right).$$

We now solve equations (4) and (5) taking into account the fact that reflected waves are absent for $x \geq l_2$. As a result, we obtain

$$\zeta_1(x) = \begin{cases} A_1\exp(ik_1x) + B_1\exp(-ik_1x) + C_1\exp(-ik_2x), & x < -l_1, \\ A_2\varphi_1(x) + B_2\varphi_2(x) + C_2\varphi_3(x) + D_2\varphi_4(x), & -l_1 \leq x \leq l_2, \\ A_3\exp(ik_5x) + C_3\exp(ik_6x), & x > l_2. \end{cases} \quad (6)$$

where

$$k_1 = k_{11}\cos\alpha, \qquad n = k_{11}\sin\alpha,$$

$$k_2^2 = k_{12}^2 - n^2, \qquad k_5^2 = k_{31}^2 - n^2, \qquad k_6^2 = k_{32}^2 - n^2,$$

$$k_{1j}^2 = \frac{H_1(\sigma^2 - f^2)}{2g\varepsilon h_1(H_1 - h_1)}\left[1 + (-1)^j\sqrt{1 - \frac{4\varepsilon h_1(H_1 - h_1)}{H_1^2}}\right],$$

$$k_{3j}^2 = \frac{H_3(\sigma^2 - f^2)}{2g\varepsilon h_1(H_3 - h_1)}\left[1 + (-1)^j\sqrt{1 - \frac{4\varepsilon h_1(H_3 - h_1)}{H_3^2}}\right], \qquad j = 1, 2. \quad (7)$$

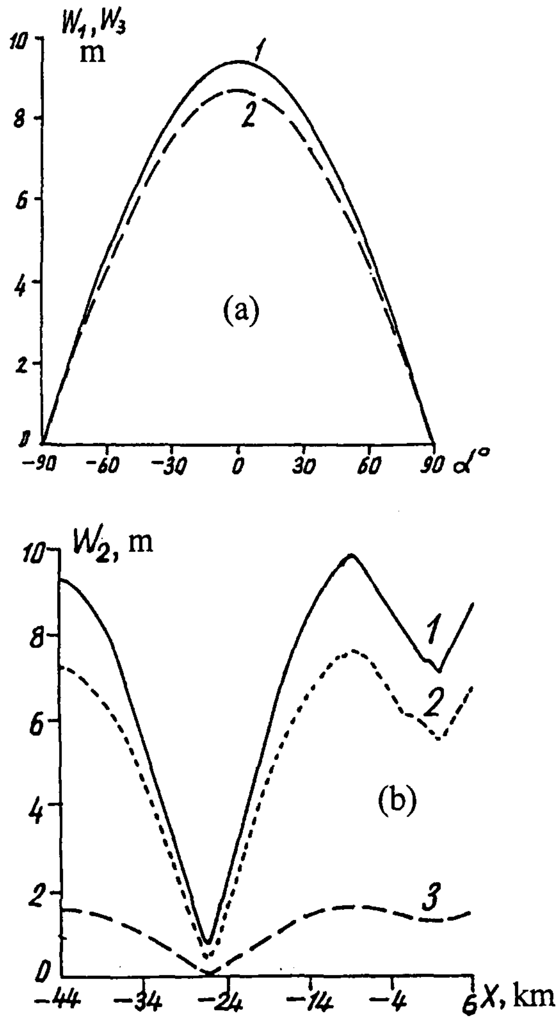

Figure 2. Amplitudes of internal waves in the first and third (a) and second (b) regions.

In relation (6), B_1, C_1, A_2, B_2, C_2, D_2, A_3, and C_3 are arbitrary constants and $\varphi_1(x)$, $\varphi_2(x)$, $\varphi_3(x)$, and $\varphi_4(x)$ is the fundamental system of solutions of equations (5) found by the fourth-order Runge–Kutta method. To determine eight arbitrary constants (the amplitude of the incident wave A_1 is regarded as known), we have eight algebraic equations expressing the conditions of continuity of elevations and flows of the fluid on the boundaries of the domains (for $x = -l_1$ and $x = l_2$). The amplitudes of waves and wave velocities are found from the numerical solution of this system of algebraic equations.

It follows from relations (6) and (7) that the form of the barotropic wave in the region $x > l_2$ strongly depends on the quantity k_5. Since $H_1 > H_3$ and $\varepsilon << 1$, we have $k_{31} > k_{11}$. Hence, for any direction of propagation of the barotropic wave (1), the quantity k_5 is real and the barotropic wave in the shallow-water region ($x > l_2$) has (qualitatively) the same form as in the deep-water region ($x < l_1$).

In view of the inequalities $k_{11}^2 << k_{32}^2$ and $k_{11}^2 << k_{12}^2$, we have $n^2 << k_{32}^2$ and $n^2 << k_{12}^2$. These inequalities and relations (7) imply that the inequalities $k_2^2 > 0$ and $k_6^2 > 0$ are true for any direction of propagation of the barotropic wave (1). Therefore, the generated internal waves cannot be entrapped. Since n^2 is small as compared with k_{12}^2 and k_{32}^2, the direction of propagation of generated internal waves is close to normal both in the first and third regions.

2. Let us now analyze the dependences of the amplitudes of waves and wave velocities on the bottom topography, stratification, and the angle of incidence of the barotropic tide for the following initial parameters:

$$H_1 = 4 \cdot 10^3\,\mathrm{m}, \quad H_2 = 3 \cdot 10^2\,\mathrm{m}, \quad H_3 = 2 \cdot 10^2\,\mathrm{m},$$

$$h_1 = 10^2\,\mathrm{m}, \quad l_1 = 4.4 \cdot 10^4\,\mathrm{m}, \quad l_2 = 6 \cdot 10^3\,\mathrm{m}, \quad \varepsilon = 2 \cdot 10^{-3}, \tag{8}$$

$$\varphi = 30^\circ, \quad A_1 = 1\,\mathrm{m}, \quad \text{and} \quad T = 12\,\mathrm{h}\,25\,\mathrm{min},$$

where T is the period of the incident wave and φ is the latitude of the location.

In Fig. 2a, we present the dependences of the amplitudes of internal waves on the interface of layers in the fluid on the angle of incidence of the tide α for the first ($W_1(\alpha)$, curve 1) and third ($W_3(\alpha)$, curve 2) regions. The maximum values of the quantities $W_1(\alpha)$ and $W_3(\alpha)$ (9.4 and 8.6 m, respectively) are attained for the normal incidence of the tide. As $|\alpha|$ increases, the amplitudes of generated internal waves in the first and third regions decrease. It is worth noting that, for the indicated parameters of the model, $W_1(\alpha) > W_3(\alpha)$ for all α.

The dependences of the amplitudes of oscillations of the interface of two layers over the unevenness of the bottom $W_2(\alpha)$ for different values of the angle of incidence are displayed in Fig. 2b. In Figs 2b, 3, and 4, curves 1–3 correspond to angles α of 0°, 40°, and 80°, respectively. In Fig. 2b, we see that, in the vicinity of the unevenness of the bottom, there are regions with high amplitudes of internal waves and regions where these amplitudes are quite low. The maximum perturbations of the interface are localized in the boundary regions of the continental slope and shelf zone ($x = -l_1$, $x = 0$, and $x = l_2$). In this case, the amplitudes of internal waves can be as high as 10 m. The minimum displacements of the interface from its nonperturbed position (0.2–0.8 m for $0 \le \alpha \le 80^\circ$) are observed in the central parts of the indicated regions. As the absolute value of the angle of incidence of the barotropic wave increases, the amplitudes of internal waves in the second region decrease.

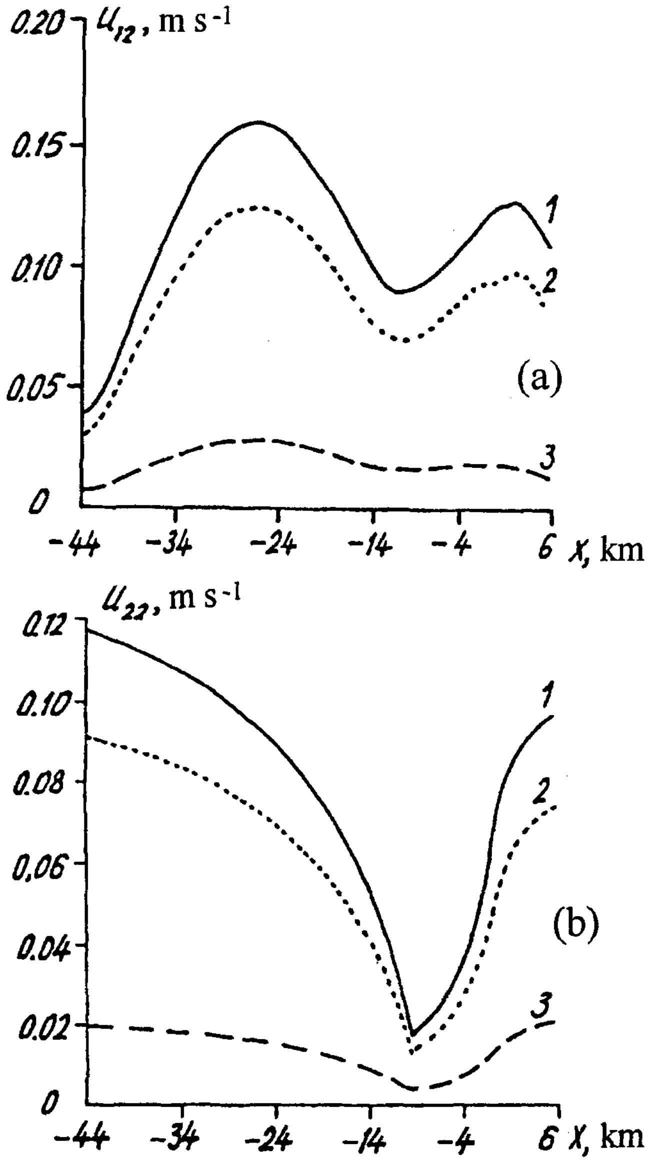

Figure 3. Amplitudes of horizontal velocities in the upper (a) and lower (b) layers.

We also performed calculations for negative values of the angle of incidence. It was shown that the values of $W_2(\alpha)$ for the angles α and $-\alpha$ differ by at most 3%.

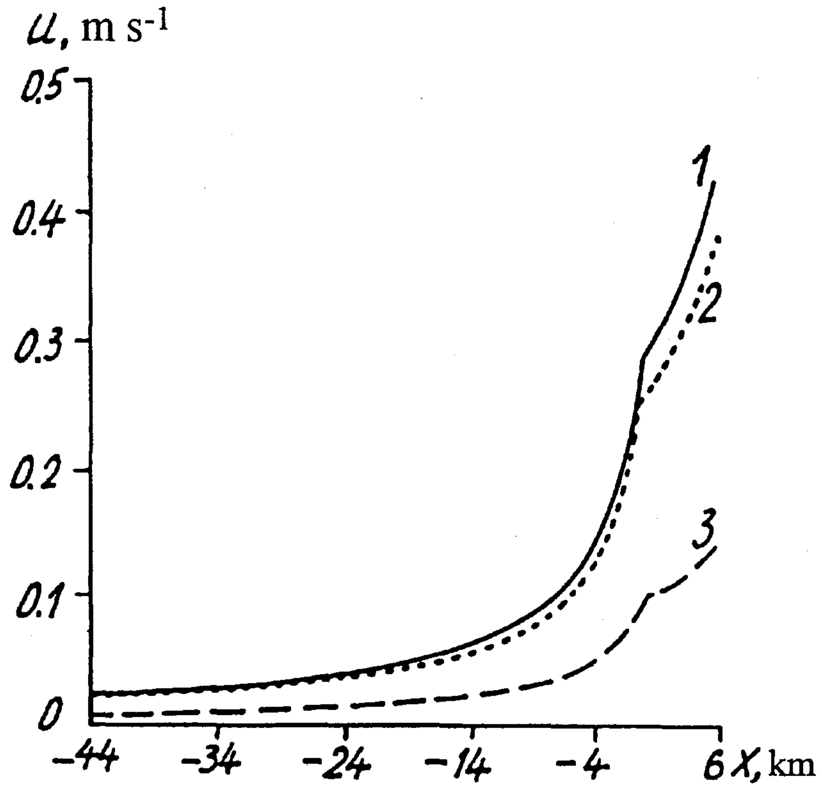

Figure 4. Amplitudes of the horizontal velocity for the homogeneous fluid.

For the second region, the dependences of the amplitudes of the horizontal component of the velocity in the upper $u_{12}(x)$ and lower $u_{22}(x)$ layers are shown in Fig. 3. As follows from Fig. 3a, the maximum velocities of wave currents in the upper layer are attained for $\alpha = 0$ in the central parts of the continental slope and shelf zone ($0.16\,\mathrm{m\cdot s^{-1}}$ for $x = -2.6\cdot 10^4\,\mathrm{m}$ and $0.13\,\mathrm{m\cdot s^{-1}}$ for $x = 2\cdot 10^3\,\mathrm{m}$) and the minimum velocities are observed on the boundaries of these regions. In the lower layer (Fig. 3b), the maximum values of $u_{22}(x)$ over the continental slope are attained on its left boundary ($0.12\,\mathrm{m\cdot s^{-1}}$ for $\alpha = 0$). In the shelf zone, the maximum values of $u_{22}(x)$ are observed on its right boundary ($0.1\,\mathrm{m\cdot s^{-1}}$ for $\alpha = 0°$). The comparison of Figs 3a and 3b demonstrates that the x-component of the horizontal velocity in the upper layer is greater than the x-component of the velocity in the lower layer over the entire unevenness of the bottom except the vicinity of its left boundary. Note that, both in the upper and lower layers, the amplitudes of velocities $u_{12}(x)$ and $u_{22}(x)$ significantly decrease in the vicinity of the point $x = -9\cdot 10^3\,\mathrm{m}$. As the absolute value of the angle α increases, both $u_{12}(x)$ and $u_{22}(x)$ decrease.

As far as the y-components of the velocity in the upper $v_{12}(x)$ and lower $v_{22}(x)$ layers are concerned, their behavior is similar to the behavior of $u_{12}(x)$ and $u_{22}(x)$, respectively. Moreover, the ratios $u_{12}(x)/v_{12}(x)$ and $u_{22}(x)/v_{22}(x)$ are equal to 2 with an error that does not exceed 10%.

We also computed the amplitudes of waves and wave velocities for two more values of the depth of the basin in the first region ($H_1 = 3\cdot10^3$ and $5\cdot10^3$ m). The values of the other parameters were the same as in (8). The analysis of the results of these calculations shows that the amplitudes of generated internal waves decrease in all three regions as the depth of the basin increases in the region preceding the unevenness of the bottom. In this case, as H_1 increases from $3\cdot10^3$ to $5\cdot10^3$ m, the maximum displacements of the interface of layers in the second region vary from 11.8 to 8.6 m (for $\alpha = 0°$). An increase in the depth of the basin in the third region also leads to a decrease in the amplitudes of generated internal waves.

3. To analyze the influence of inhomogeneity of the fluid on the field of wave velocities over the unevenness of the bottom, we also performed calculations for a model of homogeneous fluid. All other conditions were equal. For this case, the behavior of the amplitude $u(x)$ of the horizontal component of the velocity along the x-axis in the region of unevenness of the bottom is presented in Fig. 4. The comparison of Figs 4 and 3a, b demonstrates that the maximum values of the amplitudes of the velocities in the region of unevenness of the bottom decrease if we take into account the inhomogeneity of the fluid. Thus, for $\alpha = 0°$, $u_{\max} = 0.43\ \mathrm{m\cdot s^{-1}}$ for the homogeneous fluid, whereas $u_{12\max} = 0.17\ \mathrm{m\cdot s^{-1}}$ and $u_{22\max} = 0.12\ \mathrm{m\cdot s^{-1}}$. However, in this region, we observe some areas where the amplitudes of wave velocities in the two-layer fluid are higher than in the homogeneous fluid. Thus, $u(x) < u_{12}(x)$ for $-4.4\cdot10^4\ \mathrm{m} \le x \le -1.5\cdot10^4\ \mathrm{m}$ and all analyzed angles of incidence of the barotropic tide.

Thus, within the framework of the two-layer model of generation of internal waves by an "inclined" barotropic tide, we have demonstrated that, in the region of variation of the bottom topography (the continental slope and the shelf), one can find both the areas of high amplitudes of internal waves and the areas where the amplitudes of these waves are relatively small for all considered angles of incidence. The amplitudes of internal waves are maximum in the boundary regions (in the vicinity of the points $x = -l_1$, $x = 0$, and $x = l_2$) and minimum in the central parts of the continental slope and shelf. The amplitudes of the horizontal wave velocities in the upper layer attain their maximum values in the central parts of the continental slope and shelf. In the lower layer, these amplitudes are maximum on the left boundary of the continental slope and on the right boundary of the shelf.

REFERENCES

1. Baines, P. G. The generation of internal tides by flatbump topography. *Deep-Sea Res.* (1973) **20**, No. 2, 179–206.

2. Sandstrom, H. On topographic generation and coupling of internal waves. *Geophys. Fluid. Dyn.* (1976) **7**, 271–297.
3. Vlasenko, V. I. and Cherkesov, L. V. Generation of an internal tide over the continental slope. *Morsk Gidrofiz. Zh.* (1987) No. 5, 3–8.
4. Buchwald, V. T. Long waves on oceanic ridges. *Proc. Roy. Soc.* (1969) **A308**, 343–354.
5. Show, R. P. and New, W. Long-wave trapping by ocean ridges. *J. Phys. Oceanogr.* (1981) **11**, No. 10, 1334–1344.
6. Babij, M. V. and Cherkesov, L. V. Generation of internal waves by a barotropic wave in the region of an oceanic ridge. *Dokl. Akad. Nauk Ukr. SSR, Ser. A* (1982) **4**, No. 9, 49–52.
7. Dovgaya, S. V. and Cherkesov, L. V. Investigation of internal waves generated by a diurnal barotropic tide in the region of an oceanic ridge. *Morsk Gidrofiz. Zh.* (1993) No. 4, 3–12.
8. Cherkesov, L. V., Ivanov, V. A., and Khartiev, S. M. *Introduction to Hydrodynamics and the Theory of Waves.* St-Petersburg: Gidrometeoizdat (1992).